Mixing Effects on Performance and Stability of Low-Density Polyethylene Reactors

Gary J. Wells and W. Harmon Ray
Dept. of Chemical and Biological Engineering, University of Wisconsin-Madison, Madison, WI 53706

DOI 10.1002/aic.10544
Published online August 31, 2005 in Wiley InterScience (www.interscience.wiley.com).

Imperfect initiator mixing greatly affects the stability and efficiency of low density polyethylene (LDPE) autoclave reactors. A combined simulation technique utilizing compartment models and computational fluid dynamics extends previous work in the literature by providing a physically detailed picture of imperfect mixing. Analysis indicates that the effective volume for chain propagation in the autoclave reactor can expand and contract in a continuous fashion as operating conditions change. As mixing becomes poor, the effective reactive volume decreases, causing a reduction in initiator efficiency, but an expansion in the stable operation region. Examples demonstrate that accurate prediction of the effective reaction volume is crucial for predicting LDPE autoclave reactor behavior. A new mixing model that represents the feed plume by a series of interconnected tanks with geometrically increasing volumes provides a favorable tradeoff between accuracy and model complexity. © 2005 American Institute of Chemical Engineers
AIChE J, 51: 3205–3218, 2005
Keywords: mixing, stability, computational fluid dynamics, low-density polyethylene, autoclave reactor

Introduction

Low-density polyethylene (LDPE) accounts for about a quarter of U.S. polyethylene production, and is an important commodity polymer used in plastic bags, films and coatings.[1] The physics involved in the production of LDPE can be quite complex, and the reaction kinetics, polymer properties, and reactor stability in LDPE processes have, therefore, been studied for over 50 years.[2–3]

LDPE processes employ two types of reactors: (1) tubular reactors, or (2) stirred autoclave reactors, and each type of process is used extensively for LDPE production.[4] Each of these processes operates at high pressures (1,500–3,000 atmospheres), and with reactor exit temperatures ranging from about 200 to 300°C.

In this work, we model a single compact type autoclave reactor, such as the DuPont type (c.f. Figure 1). Typical processes have reactor volumes ranging between 250 and 2,000 L and residence times on the order of 10 s to one min. The heat generated by polymerization is quite high, and causes a temperature rise of about 12°C–13°C for each percent of monomer conversion.[5] Due to relatively short residence times and thick reactor walls, the capability of removing heat through wall cooling is quite low.[6] Thus, autoclave reactors can be considered adiabatic, and the exit temperature is attenuated by feeding the monomer in a cold condition.[7] Due to safety limits on the maximum temperature rise and the low residence times, single pass conversion in autoclave reactors is usually below 20%. Despite this relatively low conversion to polymer, stability issues can be a major operational concern.

At temperatures above about 300°C, a violently exothermic reaction can decompose ethylene, leading to localized dark spots in the polymer or global reactor runaway. Such ethylene decomposition reactions are common in LDPE plant operation, and occurrences of this reaction mechanism are known in the industry as a "decomp." Decomp episodes can be quite costly due to environmental and safety concerns, and can ultimately lead to significant process downtimes. LDPE autoclaves can also lose stability and migrate away from the desirable operating branch if internal temperatures drop too low and ignition

Correspondence concerning this article should be addressed to W. H. Ray at ray@engr.wisc.edu.

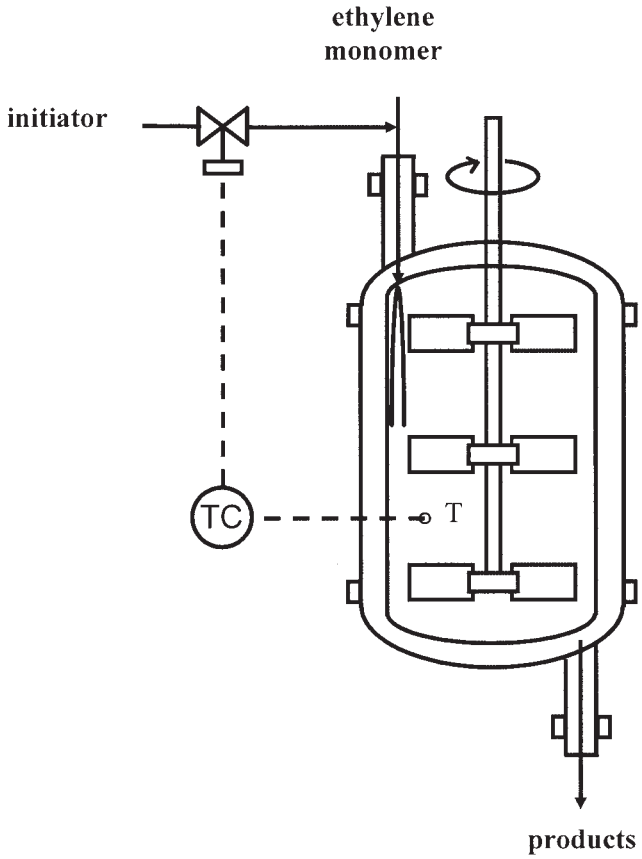

Figure 1. LDPE autoclave reactor.

of the chemical initiator is lost. This behavior leads to reactor extinction whereby the polymerization ceases. Such reactor extinction is a common industrial occurrence that causes significant production losses.

To achieve desired polymer properties and avoid extinction or runaway of the autoclave reactor, feed initiator fraction is manipulated to control a desired internal temperature. Despite the use of such controllers and high amounts of agitation energy input to the vessel, reaction conditions may not be well mixed due to the similarity of reaction and mixing time scales.[8]

In two studies led by van der Molen,[9,10] the efficiency of numerous peroxide initiators for producing LDPE in a stirred autoclave reactor was studied. It was determined that the specific initiator consumption per mass of polymer produced depended heavily on the type and intensity of mixing used in the reactor. Also, it was found that plotting this specific initiator consumption versus reactor temperature produced a minimum in the curve. This minimum was not represented using conventional kinetic modeling in a perfectly-mixed tank reactor, but it was shown that the minimum could be could be explained by imperfect mixing effects.[10]

This evidence of imperfect mixing effects in LDPE autoclave reactors led to further simulation and experimental research. Georgakis and Marini[11–13] used a three-compartment model to represent imperfect mixing of the feed stream. This model represented the feed zone by two small perfectly mixed tanks connected in series. These feed compartments were connected by flows to and from a larger perfectly mixed compartment. The major parameter of the model was the recycle rate from the large zone to the feed compartments. This recycle rate parameter was chosen to match common reactor measurements. Using this three-compartment model, Marini and Georgakis[12–13] computed conversion and polymer properties. They also computed the largest real eigenvalue for the reactor model, and found that the range of operation over which this eigenvalue was negative was expanded with imperfect mixing.

Villa et al.[14] carried out a full stability analysis of the LDPE autoclave including the effects of the decomp reactions. They showed that the perfectly mixed reactor has a tiny (or sometimes no) range of operating conditions for stable operation where polymer is produced. However, by using simple three-compartment mixing models, they predicted a broad range of productive, stable operation when there is imperfect mixing. Villa et al.[14] provide a clear physical explanation for the stabilizing effect of imperfect mixing. Their study demonstrated that small regions in the feed plume of the reactor significantly reduce initiator and radical concentrations that reach larger downstream zones. This causes a net reduction in initiator efficiency when compared to perfect mixing, and consequently reduces heat release and reactor sensitivity to temperature. Villa et al. showed that this reduction in temperature sensitivity is analogous to a stabilizing controller that reduces feed initiator concentration to the downstream zones when operating temperature increases. Subsequent studies of imperfect mixing in the LDPE autoclave have also assessed aspects of reactor operation and stability.[8,15]

Other research has examined more complex, and presumably more realistic, mixing models in the context of process efficiency and product properties.[16–20] These studies have utilized compartment mixing models of varying levels of complexity and backflow characteristics. Such models have been used to predict industrial plant data in certain operating regions, but little guidance exists concerning the appropriate level of detail required to accurately capture the effects of mixing on LDPE reactor operation.

Recently, computational fluid dynamics (CFD) has been used to provide an increased level of mixing detail in models of autoclave and tubular LDPE reactors.[21–26] Such CFD studies showed that mixing in autoclaves can play a very significant role in regions near initiator feeds, where large gradients in temperature and composition exist.[21–24] These gradients can subsequently affect process productivity and efficiency. However, due to limitations in computing power, such detailed CFD models have not been used to examine mixing effects on LDPE autoclave operation over wide ranges in feed conditions or design parameters. Furthermore, stability and polymer property issues have not been studied thus far with the level of mixing detail provided by CFD. It is envisioned that CFD will aid in understanding the underlying physics that govern mixing effects on the operation of the LDPE autoclave.

This article applies a modeling approach that combines the computational simplicity of compartment models with the mixing detail of CFD simulation. The approach models detailed mixing effects on stability and productivity in the adiabatic LDPE autoclave over wide operating ranges. General effects governing spatial variations and stability are first established in the relatively simple three-compartment model used by Villa et al.[14] and then these simple models are compared to the more detailed approach involving CFD. The analysis provides guide-

Table 1. Kinetic Mechanism for Free-Radical Homopolymerization of Ethylene

Initiation:

$$I \xrightarrow{f_{eff} k_d} 2R \quad \text{(decomposition of initiator)}$$

$$R + M \xrightarrow{fast} P_1 \quad \text{(initiation of growing chain)}$$

Chain Propagation:

$$P_n + M \xrightarrow{k_p} P_{n+1}$$

Termination by combination:

$$P_n + P_m \xrightarrow{k_{tc}} D_{n+m}$$

*Ethylene decomposition:**

$$M \xrightarrow{C_{mon}(1.89k_{md1} + k_{pd1}) + 0.0714k_{pd2}} \text{decomp products} + 30200 \text{ cal/mol}$$

*Note: Ethylene decomposition ("decomp") is modeled as a heat release only; decomp products are not explicitly tracked. This simplified form of the decomp model proposed by Zhang et al.[27] relates the rate of heat generation from monomer decomp to lumped kinetic parameters (k_{md}, k_{pd1}, k_{pd2}) from the decomposition mechanism as follows[28]:

$$R_{heat,decomp} = \Delta H_{decomp}(C_{mon}^2(1.89k_{md} + k_{pd1}) + 0.0714k_{pd2}C_{mon})$$

lines for accurately modeling the reactor over wide ranges of operating conditions, and specific recommendations are made for assessing mixing effects in industrial reactor configurations.

Reaction Kinetics

Table 1 presents the reactions comprising the kinetic mechanism used in this work for modeling free-radical ethylene homopolymerization in the high-pressure autoclave reactor. As can be seen, the common free radical initiation, propagation, and termination steps are modeled. In this work, a single chemical initiator is used, and termination is presumed to occur primarily by coupling in accordance with experimental evidence.[29]

Table 2 presents the rate constant parameters used in this study to define reactive source terms. The rate constants are assumed to be of the Arrhenius form with both temperature and pressure dependencies. A simplified form of the decomp model of Zhang et al.[27] is also applied to simulate the heat released as ethylene decomposes at high temperature.[28]

This decomp modeling approach allows reactor behavior to be accurately assessed at the upper temperature stability limit.

Table 3 shows the process parameters that are kept constant for this work unless specifically stated otherwise. The major parameters studied in this work are the feed temperature, feed initiator fraction, and reactor residence time. The initiator used is tert-butyl peroxyacetate (TBPOA), a relatively active initiator with a half life of about 2 s at 200°C. The half life of this initiator decreases significantly at higher temperatures.

Table 3. Constant Values Specified in this Work for Modeling the LDPE Autoclave Reactor*

Quantity	Value
Inlet flow velocity	50 m/s
Residence time	32.8 s
Impeller rotation rate	200 RPM
Reactor volume	500 L
Mixture density	499 g/L
Heat capacity	2.768 J/g-K
Species diffusivity	$2.88 \times 10\text{-}5$ m^2/s
Heat conductivity	0.1998 J/m-s-K
Mixture viscosity	1.6×10^{-3} kg/m-s
Initiator efficiency	1
Reactor pressure	2000 atm
Heat of polymerization	−21386 cal/mol
Heat of decomposition	−30200 cal/mol

*Note: Values for physical constants are taken from Read et al.[22]

Mixing Effects in Simple Compartment Models of the LDPE Autoclave Reactor

In the study of Villa et al.,[14] a three-compartment model (see Figure 2) was used to show that imperfect mixing expands the stable operating region of LDPE autoclaves considerably due to reduced initiator efficiency. Figure 3 illustrates these results, and also shows that at low-feed temperatures, imperfect mixing can provide a desirable stable operating branch when none exists for perfect mixing. In the figure, continuation diagrams compare the stability characteristics of perfectly mixed and imperfectly mixed models for an adiabatic reactor operating at four different feed temperatures. A residence time of 32.8 s is used, which falls in the range of industrial practice. In Figures 3a–b (feed temperatures of 420 and 400 K), one sees that stable operation is possible under both perfect mixing and imperfect mixing conditions. Although the stability region for imperfect mixing is considerably wider due to the lowered initiator efficiency, stable ignition is even possible in the perfectly-mixed case at the 32.8 s residence time. Further, at such a high-feed temperature, stable ignition is attainable for very low initiator

Table 2. Kinetic Parameters Used to Study the LDPE Autoclave*

Reaction	Units	k_0	E_A (cal/mol)	V_A (cal/atm-mol)	Source
Propagation (k_p)	L/(mol-s)	1.14×10^7	7091	−0.477	30
Initiator decomposition (k_d)	s^{-1}	1.06×10^{16}	35560	0.0605	4
Termination by coupling (k_{tc})	L/(mol-s)	3.00×10^9	2400	0.3147	30
Initial monomer decomp. (k_{md})	L/(mol-s)	4.00×10^{19}	65000	−0.1937	27
Decomp. propagation 1 (k_{pd1})	L/(mol-s)	1.59×10^{20}	65000	0.3218	27
Decomp. propagation 2 (k_{pd2})	s^{-1}	4.39×10^{20}	65000	−0.1937	31

*Rate constants (k) are computed using the formula: $k = k_0 \exp[-(E_A + V_A \cdot P)/R_{gas}T]$, where P is the absolute pressure in atm, T is the absolute temperature in K and R_{gas} is the ideal gas constant.

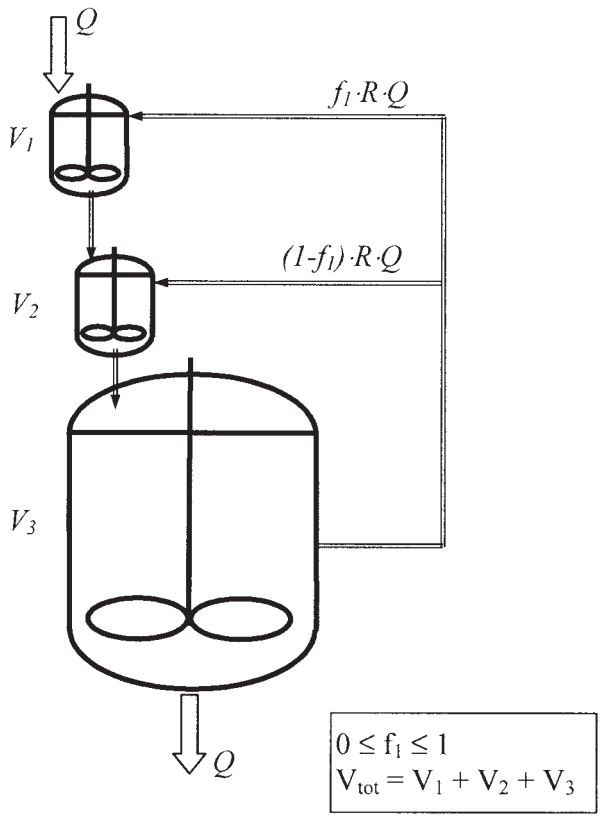

Figure 2. Three-compartment imperfect mixing used by Villa et al.[14]

Base parameters used in this work are taken from Zhang and Ray[32]: $V_1/V_{tot} = 1/24$, $V_2/V_{tot} = 2/24$, $f_1 = 1/3$. The recycle ratio R is varied.

feed fractions because the feed stream itself has enough energy to support ignition of the entire reactor volume.

At the lower feed temperatures of 360 K and 300 K (Figure 3c–d), imperfect mixing provides a desirable stable operating branch, but no such stable conditions exist for the perfectly-mixed model using the TBPOA initiator at the current residence time. For these lower feed temperatures, a significant temperature rise in the partially isolated feed zone must occur in tandem with backmixing of hot material to decompose the initiator and ignite the reactor. These conditions are provided by the three-compartment imperfect mixing model, but not by the perfectly-mixed model.

It should be noted that low feed temperatures in the range of about 293–363 K (20–90°C) are common industrially,[33] because they allow for greater adiabatic temperature rise and higher monomer conversion before the dangerous decompositions reactions become important. Thus, the results of this section emphasize the necessity of including mixing effects in models of industrial LDPE autoclave reactors, since perfectly-mixed models may not predict any desirable stable branch for industrially relevant values of feed temperature and residence time.

Effect of internal flows in adiabatic reactor operation

In this section, the effects of internal flow rates on the spatial uniformity and efficiency of the LDPE autoclave reactor are examined for the three-compartment model of Figure 2. To influence the internal flows, the recycle ratio (R) is varied. Higher values of R indicate more vigorous internal flows and reduce the local flow time scales in an approximately linear fashion. Lower values of R indicate correspondingly less vigorous internal flow. Values of R between about 2 and 20 have been used to fit measured data for industrial LDPE autoclave reactors.[12]

For adiabatic reactors models such as that considered in this section, the initiator half life is dependent on recycle ratio (or local compartment residence times) through its influence on local temperatures. Since initiator dispersion is the primary factor that determines the degree of mixing in LDPE autoclave reactors, such temperature variations have the potential to provide much more complicated behavior than observed under isothermal conditions. Indeed, it is shown in this section that increasing recycle ratio does **not** always decrease spatial variation in radical concentration or polymerization reaction environment within the range of stable operation. This nonintuitive behavior is explained using the simulation examples presented later.

Figures 4a through 4d show the effect of recycle ratio on several important quantities for the standard adiabatic three-compartment model with a 300 K feedstream containing 50 ppm of the TBPOA initiator. Under these conditions, there are both upper and lower limits for stability as recycle ratio (R) is varied. At values of $R < 5$, the reactor will extinguish because insufficient heat is mixed back into the feed zone to achieve a stable amount of free radical generation. At values of R greater than about 210, the entire reactor will reach the conditions of global monomer decomposition. In between these stability limits, significant changes in internal conditions and kinetic rates occur. As recycle ratio is increased from the lower stability limit to the upper stability limit, the temperature and bulk

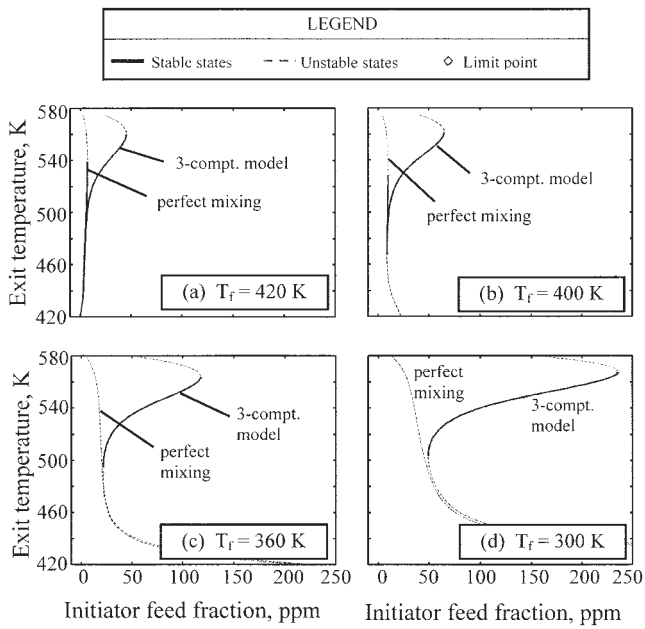

Figure 3. Stability diagrams comparing perfectly mixed and imperfectly mixed models.

A residence time of 32.8 s is used. Plots: (a) $T_f = 420$ K, (b) $T_f = 400$ K, (c) $T_f = 360$ K, (d) $T_f = 300$ K.

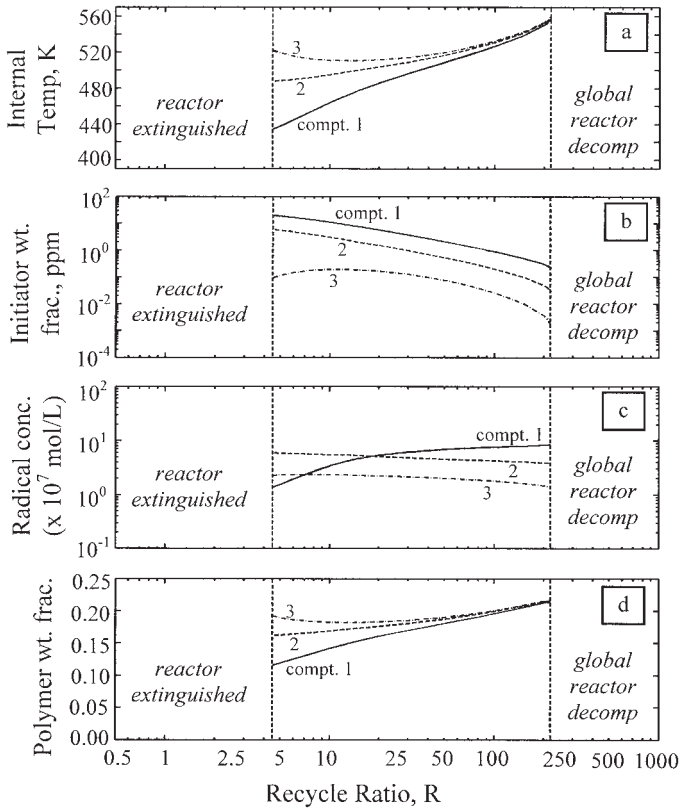

Figure 4(a–d). Effect of recycle ratio on spatial variations of temperature and composition.

An adiabatic, 3-compartment model is used with feed conditions of 300 K and 50 ppm of the TBPOA initiator.

polymer fraction both become more uniform in space. Two interrelated effects work to increase uniformity of bulk polymer fraction and temperature with increasing R: (1) increased back-mixing of hot material raises the feed zone temperature, such that it approaches the temperature of downstream zones, and (2) the feed zone produces an increasing amount of polymer/heat that is passed on to the downstream zones.

In contrast to what is seen for polymer content and temperature, Figure 4c shows that radical concentrations vary in the three zones by over an order of magnitude despite increased internal flows. As the temperature of zone 1 increases due to increased back-mixing, the initiator half-life decreases in an exponential fashion. In contrast, the flow-time scale decreases with R more slowly, in an approximately linear fashion. As a result, the initiator is consumed to a greater extent in the feed compartments as R is increased (see Figure 5a), and significant spatial variations in initiator and radical concentrations result. Furthermore, as the recycle ratio is increased, the higher temperatures and radical concentrations in zone 1 cause it to produce a much larger portion of the total conversion than it would under perfectly mixed conditions (see Figure 5b). Clearly, if very high recycle ratios were attainable on the stable operating branch, the radical concentrations in the reactor would eventually become spatially uniform. However, in the stable range of operation, spatial uniformity of radicals is not improved with stirring rate due to the influence of temperature on initiator half-life.

As shown in subsequent sections, operating conditions influence reactor uniformity and efficiency much more than internal flows. Therefore, design parameters such as feed initiator fraction, feed temperature, and residence time are the focus of highly-detailed mixing model studies in the subse-

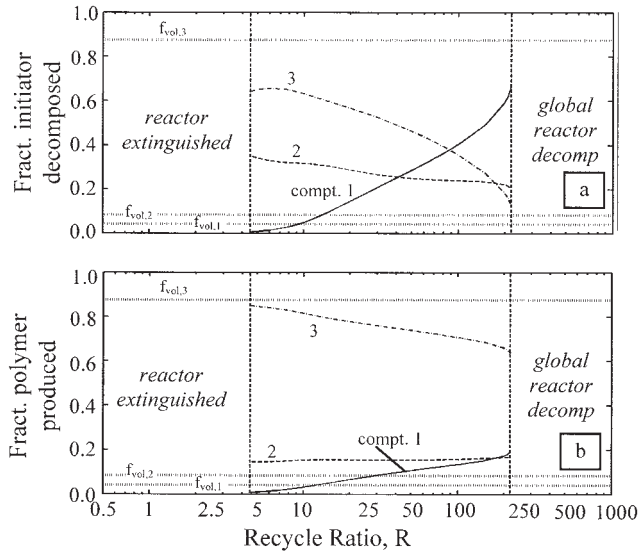

Figure 5(a–b). Effect of recycle ratio on fractional conversion and initiator consumption in each compartment.

The feedstream is introduced at 300 K with 50 ppm of the TBPOA initiator.

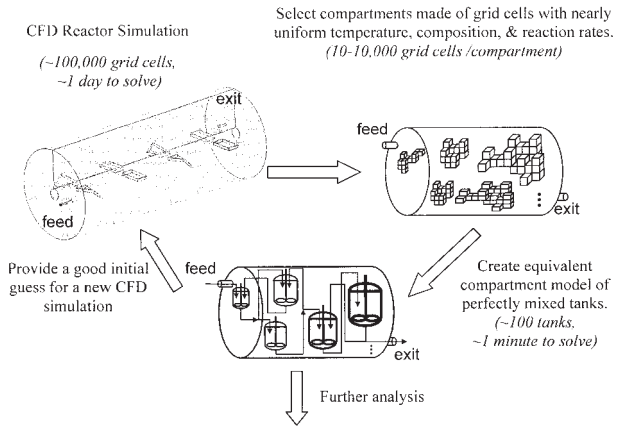

Figure 6. Procedure for selecting and using a compartment model of the LDPE autoclave reactor.

quent sections. Additional details on the effect of internal flows on reactor performance may be found elsewhere.[28]

Detailed Modeling of Mixing and Reaction in the LDPE Autoclave

Because spatial variations of the active radical species and initiator are difficult to measure in the LDPE autoclave, experiments cannot easily provide a visual picture of how these species are mixed. Simple compartment models have shown that the spatial variations of these quantities are extremely important in determining reactor operation.[12–14,22,34] Although simple compartment models can be used to match industrial measurements, there is no guarantee that simple models accurately capture mixing details under all conditions, especially since the initiator efficiency or kinetic rate constants are often varied to fit the data.[18,35] If mixing details are not properly represented, such simple models may not extrapolate well to conditions outside of the experimental range. Furthermore, as discussed by Smit,[36] any model that captures some degree of incomplete mixing can represent experimental measurements such as the nonideal behavior of initiator consumption under imperfect mixing. Therefore, in order to properly model the physics of reactor mixing, it is desirable to know *how much* mixing detail is necessary to accurately represent LDPE autoclave reactor behavior over a wide operating range.

CFD simulation and equivalent compartment model

This work assesses the appropriate level of mixing detail for accurate modeling of the LDPE autoclave by reducing a CFD model with a great deal of mixing detail to obtain an equivalent, simpler compartment model. The CFD/compartment model approach involves a precise representation of spatially varying temperature and compositions fields, and can be applied generally to many processes. Specific details of this methodology are provided elsewhere,[37] but the basic concept and application in the case of LDPE autoclave reactor modeling is presented in Figure 6.

The combined CFD/compartment model approach starts from a single, converged reactive CFD simulation. In the current case, the LDPE autoclave reactor is modeled using the Fluent CFD package,[38] and a reactor design from Read et al.[22] that is chosen to match typical industrial autoclaves. Due to the high level of agitation common in LDPE autoclaves, the flow is modeled as fully turbulent. Constant density and viscosity are assumed since the conversion is about 20% or less, and these physical properties in the supercritical mixture are similar to those of liquid water.[16] The CFD mesh is shown in the upper lefthand corner of Figure 6, and involves about 100,000 grid cells to represent the 500 L reactor volume. Wherever possible, model parameters such as vessel geometry, reaction kinetics, and feed conditions are taken from the literature. CFD results for initiator consumption, exit conversion, and adiabatic temperature rise have been confirmed to be in the operable range for industrial reactors.[4,6,10]

Once a single reactive CFD simulation is converged at a base set of operating conditions, an equivalent compartment model is selected to represent the reactive flow field in a simplified way. The 100,000 grid cells in the base CFD simulation are subdivided into numerous grid cell groupings in order to make the zones represented by the groupings uniform in temperature, composition, and the important reaction rates such as chain propagation and termination. Each of these grid cell groupings is represented as a perfectly-mixed reactor in a compartment model of interconnected tanks. The zone volumes are taken to be the sum of the grid cell volumes that comprise that zone, and the interconnecting flows are also taken from the base CFD simulation. The compartments that result from this subdivision procedure can be of various shapes and sizes, and they generally follow the composition and temperature gradients that exist in the reactor. The flows between compartments also mimic the dominant circulation patterns determined by the CFD simulation.

The procedure that constructs the compartment model from CFD output files has been automated and can handle an arbitrary number of compartments. Although stability of a single-stage LDPE autoclave reactor has been considered here, the methodology can be also be applied to more complex vessels such as multi-stage autoclaves. The specific criteria used in the compartment model selection may be found in Wells[28] and Wells and Ray.[37] Typically, about 100 perfectly-mixed tanks are needed to represent the temperature and composition gradients that exist in the reactor. A single set of compartment model selection criteria can be applied to accurately represent CFD results over a wide operating range, and the computational simplicity of the selected compartment models allows them to be computed up to 1,000 times faster than the full CFD simulations. As a result, the compartment models can be used in stability analysis or other computational techniques where full CFD simulations would be difficult or impossible to apply. In subsequent sections, the compartment model/CFD approach provides a detailed view of LDPE autoclave reactor mixing and its effects on reactor performance and stability.

Quantification of effective volume usage and initiator efficiency

This section defines numerical quantities that will be used throughout this article to compactly represent the degree of vessel mixing and reactor efficiency. These values are not model parameters, but are instead quantities used to assess mixing thoroughness based on converged simulation results.

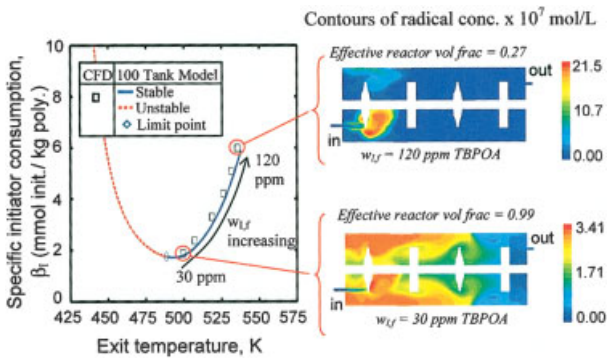

Figure 7. Mixing effects on initiator efficiency.

A feed temperature of 360 K and a residence time of 32.8 s are used. Contours are shown on a plane that cuts through the 3-D reactor volume by intersecting the inlet pipe, outlet pipe, impeller shaft, and impeller blades. The effective reactor volume fraction is shown for $\alpha = 0.05$. The base CFD case for the 100-compartment model is for a feed of 360 K and 120 ppm TBPOA.

One such measure for quantifying the effective reactor volume can be defined as follows

$$f_{rV}(\alpha) = \frac{\sum_{i=1}^{n_{\text{zones}}} V_i \cdot H(R_{p,i} - \alpha \cdot R_{p,\max})}{\sum_{i=1}^{n_{\text{zones}}} V_i} \tag{2}$$

Here, H is the unit step function, and $f_{rV}(\alpha)$ is the effective reactor volume fraction, that is, the fraction of the reactor volume actually used for reaction dependent on the choice of "use" parameter α. Values of α in the range from 0.05 to 0.10 seem reasonable. The value V_i represents the volume of a particular zone i measured in liters, and $R_{p,i}$ is the polymerization rate (mol/L-s) in that zone. Zones can be either a perfectly-mixed tank in a compartment model or an individual grid cell in a CFD simulation. $R_{p,\max}$ is the maximum polymerization rate that occurs throughout all reactor zones. Thus, for $\alpha = 0.05$, the value of $f_{rV}(\alpha)$ is the fraction of the reactor volume that is utilized for producing polymer at a rate greater than 5% of the maximum. Generally, values of f_{rV} close to one indicate good reactor mixing. Conversely, values of the measure near zero indicate very poor mixing. For perfectly-mixed reactors, f_{rV} will always be unity, although a value $f_{rV} = 1$ can also occur in reactors with a small degree of imperfect mixing.

In addition to the reaction volume effectiveness measure defined earlier, the classic measure of initiator consumption reported by van der Molen et al.[10] can be used to provide significant insight into imperfect mixing effects

$$\beta_I = \frac{10^6 \cdot w_{I,f}}{x_p \cdot MW_I} \tag{3}$$

Here, $w_{I,f}$ is the initiator feed fraction, x_p is the monomer conversion, and MW_I is the initiator molecular weight. The value of β_I is the amount of initiator required to produce polymer, and is typically defined as earlier in units of mmol of initiator per kg of polymer produced. This quantity can be considered as an inverse measure of initiator efficiency.

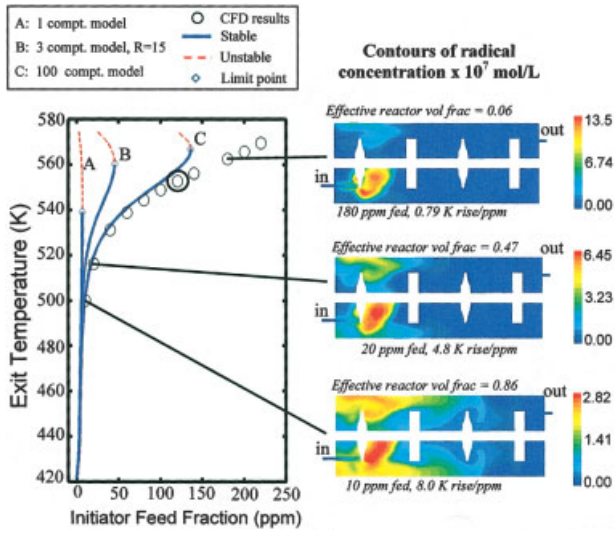

Figure 8. Effect of initiator feed fraction on reactor exit temperature and stability range.

$T_f = 420$ K, residence time = 32.8 s. The effective reactor volume fraction is shown for $\alpha = 0.05$. The base CFD case for generating the 100-compartment model is the circled point with a feed stream at 420 K and 120 ppm of TBPOA.

Mixing effects on initiator consumption

Figure 7 shows the specific initiator consumption curve of the form used by van der Molen and coworkers to describe initiator efficiency.[9–10] The points along the curve represent different amounts of initiator in the feed, and radical concentration contours in the reactor are presented at two of these points. The contour graphs are shown for a cutting plane in the

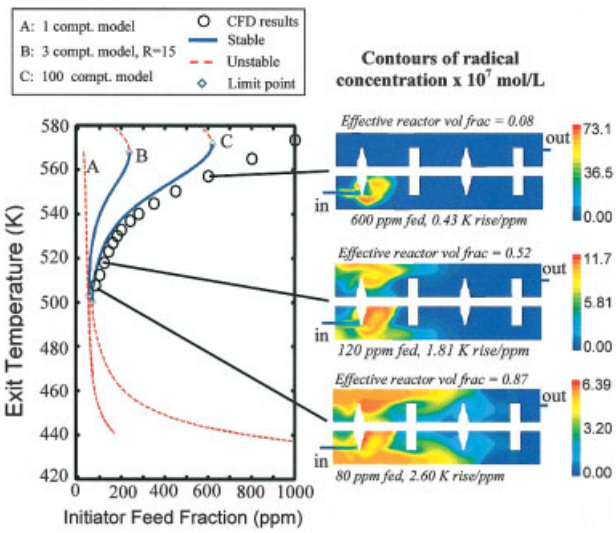

Figure 9. Effect of initiator feed fraction on reactor exit temperature and stability range.

$T_f = 300$ K, residence time = 32.8 s. The effective reactor volume fraction is shown for $\alpha = 0.05$. The base CFD case for generating the 100-compartment model involves a feed stream at 420 K with 120 ppm of TBPOA.

reactor that intersects that feed and exit pipes, as well as the impeller and stirring blades. From continuation and stability analysis of the compartment model, the region of stable operation is also determined.

As in the studies of van der Molen et al.,[9–10] the current analysis shows that the initiator consumption has a minimum at an intermediate internal operating temperature. This behavior can be understood by examining the two radical contours. At the higher amount of initiator in the feed (120 ppm), the total polymer production is also higher, and the adiabatic reactor exit temperature is about 535 K. At this temperature, the initiator half-life is short compared to flow timescales, and the initiator is poorly dispersed. This poor initiator dispersion can be seen from the radical concentration profile shown for the high initiator feed fraction. Due to the poor initiator dispersion, the radicals are concentrated near the feed region, and the bimolecular termination reaction destroys many radicals before they can add significant monomer to form polymer. Also, only about 1/4 of the reaction volume is effectively used in the polymerization reaction. This causes the initiator consumption per kilogram polymer produced to be quite high, increasing production costs.

Conversely, at a much lower initiator feed fraction of 30 ppm, the operating temperature drops considerably to about 500 K. At this temperature, the initiator half-life is similar to flow time scales, and initiator is dispersed relatively evenly. As a consequence, radicals are present in most of the reactor, the bimolecular termination reaction is less dominant, and the reactor volume is used effectively in polymerization. This behavior is consistent with the better initiator usage, meaning that less initiator is used per kilogram of polymer produced. Unfortunately, as can be seen in Figure 7, the conditions for the best radical dispersion and lowest specific initiator consumption are also near the reactor extinction limit. As a result, reactor operation requires a tradeoff between efficiency of initiator usage and robust process stability.

Effect of feed conditions on mixing and stability

The visual picture of mixing and its relationship to stability is further explored in Figure 8. In this figure, continuation diagrams show the effect of initiator feed fraction on exit temperature for different feed temperatures. Several models with varying levels of mixing detail are compared. The stability limit for global reactor decomp is shown along with radical concentration profiles for selected points along the curves. CFD simulation results (discrete points) are presented for all operation conditions that would converge in Fluent to a stable solution at the given feed temperature. Thus, the discrete CFD results represent the stability range obtained using the fully-detailed model, and these results can be used for comparison to the stability range predicted by other models.

As can be seen in Figure 8, there is only one stability limit point at high temperatures due to monomer decomposition for the feed temperature of 420 K. For this feed temperature and the TBPOA initiator, the feed stream itself is hot enough to maintain ignition without any significant back-mixing. Thus, a region of stable operation exists with reasonable conversion for each model type; however for perfectly mixed reactors, the stable region is too narrow to be practical, while stable reactor operation is feasible for imperfect mixing. Note that, as expected, the 100-compartment model more closely predicts the exact range of stable operating conditions (from CFD) than the three-compartment model with unfitted parameters. Also the reasonable fit to the CFD results observed for the 100-compartment model in Figure 8 is related to initiator dispersion and wastage. In the case of low initiator feed concentrations ($\sim$10 ppm), the feed zone reaction rates and temperature are low, resulting in long initiator half-lives. This allows time to disperse the initiator and radicals throughout the reactor. Thus, the volume usage and mixing of the reactor is quite good at low initiator feed rates and operating temperatures, and all models yield similar results. As more initiator is fed, the total polymerization rate and operating temperature increase, initiator half-life decreases, and radical dispersion worsens. At 20 ppm of initiator feed, for instance, only about half of the reactor contains radical concentrations significant enough to produce reasonable amounts of polymer. For 180 ppm of initiator in the feedstream, higher feed zone reaction rates and temperatures cause the initiator and radicals to be even more concentrated in the feed zone, reducing effective volume usage to below 10%.

The increase in initiator wastage that is observed with increasing initiator feed is a significant stabilizing effect, similar to that seen previously. These results show that the exit temperatures of the more detailed models are less sensitive to initiator feed fraction than the simpler models. For this reason, the predicted stable region is much broader in the detailed models. At the highest initiator feed fractions, even the 100-compartment model cannot match the CFD simulations precisely. This disparity results from the base CFD case (at 120 ppm of feed initiator) from which the compartment model was generated. This particular base case does not represent the poorest mixing conditions well because compartment volumes near the feed are not small enough to represent the very high gradients in radical concentration present under those poorly mixed conditions. Using additional base CFD simulations at high feed initiator concentrations can bring the resulting 100-compartment models much closer to the CFD results in this range of initiator levels. Nevertheless, the compartment model based on only one CFD case performs well in the range of practical operation, since exit temperatures exceeding about 555 K are generally avoided industrially due to the threat of decomp.[39]

Figure 9 shows the analogous stability diagram for a 300 K feed stream. The lower feed temperature introduces an additional low temperature stability limit point at reactor extinction. Therefore, at the lower feed temperature of 300 K, perfect mixing models do not yield a desirable, stable operating branch for the given residence time. For imperfect mixing, the unfitted three-compartment model indicates a desirable, stable operating region, but the range is not as broad as that predicted by the CFD model. The 100-compartment model, however, closely matches the range of stable operating conditions observed from the CFD simulations at exit temperatures below about 555 K (282°C), a reasonable upper limit for autoclave reactor operation that avoids the threat of monomer decomp. As before, using additional CFD base cases at higher initiator feed concentrations will improve the resulting 100-compartment models in this range.

We have shown that feed initiator fraction has a very significant effect on adiabatic reactor operation and degree of mixing. In addition, Figure 10 shows that feed temperature also

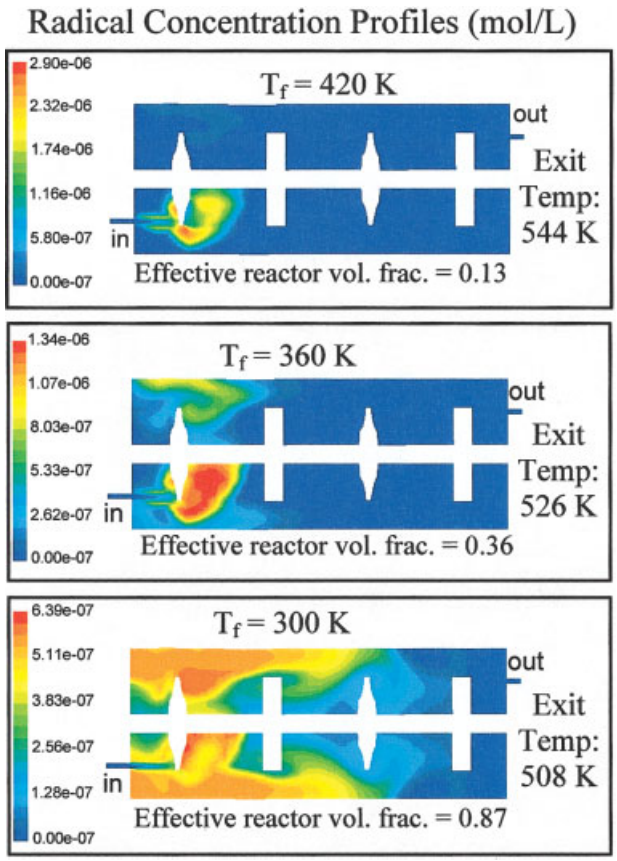

Figure 10. Effect of feed temperature on radical concentration profiles.

The initiator feed fraction is 80 ppm TBPOA and the residence time is 32.8 s. The effective reactor volume fraction is shown for $\alpha = 0.05$.

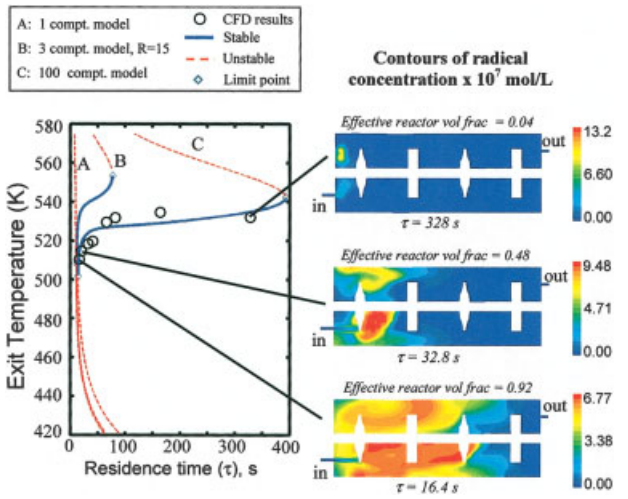

Figure 11. Effect of residence time on reactor exit temperature and stability range.

$T_f = 360$ K, $w_{I,f} = 60$ ppm TBPOA. The effective reactor volume fraction is shown for $\alpha = 0.05$. The base CFD case for generating the 100-compartment model involves a feed stream at 420 K with 120 ppm of TBPOA.

can significantly affect radical dispersion at a fixed initiator feed fraction (80 ppm). Higher feed temperatures significantly increase the initiator decomposition rate in the feed zone. The resulting decreased initiator half life leads to poorer initiator and radical dispersion and less efficient volume usage. Thus, from the standpoint of radical dispersion, the effect of increasing feed temperature at fixed initiator feed is similar to that seen when initiator feed is increased at a fixed feed temperature.

Effect of reactor residence time

Figure 11 shows the effect of reactor residence time on radical dispersion and reactor stability for a feed temperature of 360 K, and a feed initiator fraction of 60 ppm TBPOA. The perfectly mixed reactor has no stable steady state except at near-zero conversion or global reactor decomposition. The unfitted three-compartment model predicts a relatively narrow region of stability compared to the more exact CFD results; however, the 100-compartment model technique represents the stable region quite well.

The radical concentration profiles illustrate that residence time plays a large role in radical location. At the lowest residence time (16.4 s), the exit temperature is such that the initiator and radicals can disperse well throughout the reactor, leading to efficient volume usage. As residence time increases from 16.4 s to about 100 s, more reaction is allowed to take place and the exit temperature and monomer conversion increase accordingly. However, at residence times greater than about 100 s, the exit temperature becomes relatively insensitive to further residence time increases. This occurs because mixing becomes extremely poor at high residence times, and longer residence times only expand the unused portion of the reactor. This conclusion is supported by the radical concentration pro-

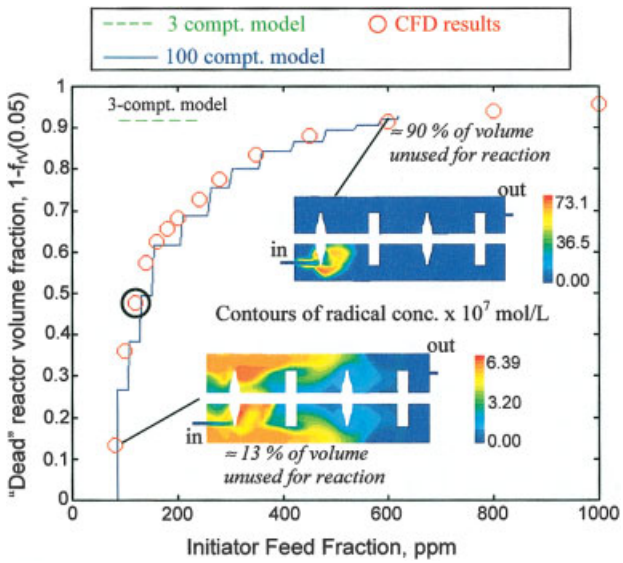

Figure 12. Fraction of unused volume as a function of initiator feed fraction.

The feed temperature is 300 K, and the reactor residence time is 32.8 s. The base CFD case for generating the 100-compartment model involves the circled point for a feed stream at 300 K with 120 ppm of TBPOA.

files, which show only a very small volume being used for reaction at the highest residence time (328 s).

Requirements for accurate LDPE autoclave reactor models over wide operating ranges

To accurately capture the stability region for LDPE autoclave reactor operation, a model must be able to predict the correct heat generation over the operating range of interest. As was shown in the previous sections, heat generation is largely dependent on the effective volume for polymerization. As initiator feed rate, feed temperature, or residence time is increased, a decrease in effective volume is a significant stabilizing force. A three-compartment model can vary the effective volume over a fairly large range by allowing temperature to vary spatially and by distributing radicals amongst the zones. However, for a fixed selection of the three-compartment model parameters, the effective volume cannot drop below the smallest compartment volume. Furthermore, once a three-compartment model is parameterized, the volumes in which significant reaction occurs can only change very discretely. This situation can be improved by selecting new three-compartment model parameters for different conditions, but if prediction of unknown operating conditions is desired, it is difficult to accurately select these parameters.

In contrast, the 100-compartment/CFD modeling technique can vary the volumes of reaction in a nearly continuous manner, and this volume variation occurs automatically as the relative time scales for fluid motion and reaction change. Thus, fitting the observed physical reaction volume requires no change in model parameters, in contrast to the three-compartment model approach. Figure 12 examines this advantage of the 100 compartment/CFD strategy over the simple 3-compartment model approach. The "dead" volume is plotted for the various models as initiator feed fraction varies at a feed temperature of 300 K. In this case, the "dead" volume fraction $(1 - f_{rV}(0.05))$ is considered to be the portion of the reactor with polymerization rates less than 5% of the maximum polymerization rate. Using this measure, one sees that the dead volume in the CFD simulations increases continuously as initiator feed fraction is varied in the stable range. This continuous variation in dead volume can be visualized by radical concentration gradients shown in the contour graphs for selected points.

Although the 100-compartment model is clearly discrete in nature, it matches the dead volume variation of the CFD simulation quite well for all but the highest initiator feed fractions, where exit temperatures approach the decomp limit. In contrast, the three-compartment model does not match the stability region or the dead volume fraction well. For this low feed temperature of 300 K, the three-compartment model has a large maximum in radical concentrations in the second zone, with low polymerization rates in the first and third zones that fall below the 5% threshold. Thus, for the three-compartment model parameters chosen, the "dead" volume fraction of the three-compartment model is about 0.92 for the entire stable region.

From the results presented in Figure 12, it appears that success in predicting the proper stability region requires the model to vary the "dead" reactor volume. For this reason, it is interesting to consider the development of simple alternatives

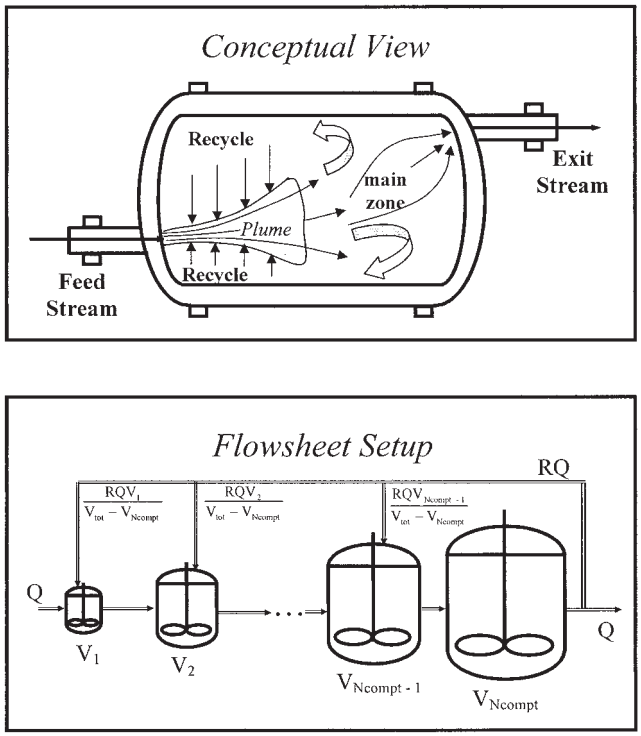

Figure 13. Simplified model for representing a geometrically-expanding plume region.

The compartment volumes are defined as: $V_i = V_1\ \lambda^{i-1}$, where the growth factor λ is fixed for this work at $\lambda = 1.2$. Note that $V_{tot} = \sum_{i=1}^{N_{compt}} V_i$.

to the three-compartment model that retain the volume variation of highly detailed models but do not require CFD simulation. A proposed modeling strategy to achieve this goal is illustrated in Figure 13.

The simplified model presented in Figure 13 consists of a sequence of perfectly-mixed reactors with recycle much like the three-compartment model technique. However, many more volumes are included to represent a plume that can shrink or grow as the initiator half-life changes. Furthermore, the tanks in the sequence increase geometrically in size as they move away from the main feed, allowing for a wide range of effective reaction volumes. This modeling strategy is designed to physically represent a feed plume that engulfs additional fluid as it progresses down the reactor.

The model illustrated in Figure 13 is similar in its physical representation of the flow to the plume engulfment model proposed by Zwietering.[40] The plume engulfment model has been applied to general reactive mixing problems, and considers incoming fluid volumes to have varying "ages." Fluid volumes that have just entered the reactor are "young," and become closer to the bulk conditions as their age increases. Unfortunately, the method of Zwietering requires the estimation of age time constants that may be difficult to obtain.

In contrast to the Zwietering mixing model,[40] the plume model presented in Figure 13 involves a more convenient stirred-tank representation and is relatively simple to formulate. The plume model has only three parameters: the number of compartments $N_{compt.}$ the recycle ratio R, and the factor λ which describes the geometric rate of increase of compartment

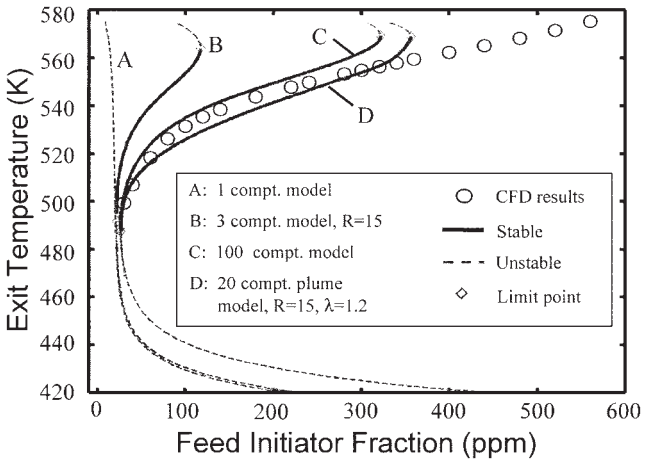

Figure 14. Comparison of the plume model to other model formulations.

The effect of initiator feed fraction on exit temperature is shown for feed temperature of 360 K. The base CFD case for generating the 100-compartment model involves a feed stream at 420 K with 120 ppm of TBPOA.

volumes along the reactor train. The rate of side feed to the reactors from the recycle stream is proportional to the volume of the receiving compartment. This new simplified model could be parameterized by knowledge of plant data, similar to the three-compartment model approach. However, the plume model also has the ability to expand and contract its physical region of reaction nearly continuously and automatically as conditions change, similar to the 100 compartment/CFD methodology.

The plume model presented here represents a straightforward approach that can be applied in practice, and it is expected to capture the stability region more completely than the simpler three-compartment model. This hypothesis is confirmed in Figure 14, which compares the performance of the plume model (for $\lambda = 1.2$, $R = 15$, and 20 zones) to that of the three-compartment model, the 100 compartment model, and CFD data. As can be seen from this figure, the plume model captures a span in the stable region that is similar to the 100-compartment model. In general, the plume model performs quite well given its simplicity, but it does not provide the same level of spatial detail as the 100-compartment model. Other advantages and disadvantages of the various modeling approaches employed here are summarized in Table 4, and should be considered when modeling the operation of LDPE autoclave reactors.

In general, because of its relative simplicity, good accuracy, and ease of parameterization, the new plume model may represent a good compromise between effort and accuracy when simulating the LDPE autoclave reactor. The plume model may be especially attractive if a CFD model has not yet been developed for the reactor, since model setup is often the most time-consuming part of the overall CFD simulation process.[41]

Summary and Conclusions

In this work, analysis using both simplified and detailed models emphasizes the importance of including mixing effects in models of adiabatic LDPE reactors. In agreement with previous research, results show that perfectly-mixed reactors have much narrower stable operating regions than imperfectly-mixed reactors. At lower feed temperatures and residence times, perfectly-mixed reactors can have no desirable stable operating branch, in contrast to imperfectly-mixed reactors with the same feed conditions. In adiabatic operation, the extent of stirring or recycle flow can affect the internal reactor temperature fields, and can, therefore, have a very large effect on both the flow and the reaction time scales throughout the reactor. Simple three-compartment models show that a range of stable recycle ratios can exist in the LDPE autoclave reactor, and for many feed conditions, no amount of stirring can make

Table 4. Comparison of Models for LDPE Autoclave Reactors

Model I—Perfect mixing:
Advantages:
- Very simple and fast computation, including stability analysis
- No adjustable flow/volume parameters
- Does not require knowledge of the flow field

Disadvantages:
- Does not offer stabilization from poor initiator usage or variable effective reaction volume
- Very limited stability region

Model II—Three-compartment model technique:
Advantages:
- Simple and fast to compute, including stability analysis
- Includes the stabilizing effect of poor initiator mixing, greatly expands stability region compared to perfect mixing
- Only requires rough knowledge of flow field

Disadvantages:
- Only designed to represent poor mixing in feed zone
- Requires choice of free parameters for flows/volumes
- Lacks ability to have variable downstream volume wastage; can significantly underestimate initiator wastage and range of stable operating conditions

Model III—CFD:
Advantages:
- Most general method for representing reactive mixing
- Provides great spatial detail
- Includes the stabilizing effect of poor initiator mixing as well as variable effective reaction volume; more accurately represents feasible operability range
- No free parameters for flows and volumes

Disadvantages:
- Time consuming to set up and compute; difficult to use in stability analysis
- Requires detailed knowledge of reactor geometry

Model IV—Combined CFD/Compartment model:
Advantages:
- Retains spatial detail of CFD solution
- Accurately represents stability region
- Much faster than CFD, allowing stability analysis
- No free parameters for flows and volumes

Disadvantages:
- Requires at least one CFD simulation or detailed knowledge of flow/reactive field

Model V—New plume mixing model:
Advantages:
- Can represent stability region fairly well
- Simple to compute, allowing stability analysis
- Does not require CFD or detailed knowledge of flow/reactive field

Disadvantages:
- Loses some knowledge of spatial details
- Requires specification of free parameters for flows/volumes

radical concentration uniform in the desirable stable operating region.

Models of the LDPE autoclave reactor using a combined compartment model/CFD approach provide a great degree of spatial detail, and also reproduce the stable operation region with a high degree of accuracy. Such detailed models allow the effective reaction volume for polymerization to vary continuously as feed conditions are changed. Lower feed temperatures and initiator feed fractions provide the highest degree of uniformity in initiator and radical concentration. Such uniform conditions result in the most efficient volume usage for reaction and the highest initiator efficiency in producing polymer. However, obtaining such efficient conditions requires operation near the stability limit for reactor extinction.

Analysis of several different models shows that the variation in effective volume usage is key to capturing the broad stability range observed in CFD simulations. On the basis of this knowledge, this article proposes a new simplified imperfect mixing model of the LDPE autoclave that represents the feed plume as a series of interconnected compartments with geometrically increasing volumes. The plume model captures the wide range of stable operation observed in CFD simulations. Furthermore, no fitting to CFD simulations is required, and yet the predictions are quite close to the CFD results. Thus the plume model may represent a good tradeoff between computational effort and accuracy.

Acknowledgments

The authors are indebted to the industrial sponsors of the University of Wisconsin Polymer Reaction Engineering Laboratory, and to the U.S. Department of Energy for financial assistance. We also thank Iasson Mustakis and Carlos Villa for their insight and support.

Notation

CFD = computational fluid dynamics
C_{mon} = monomer concentration, mol/L
C_p = heat capacity of mixture, cal/(g-K)
D_n = dead polymer chain of length n monomer units
E_A = activation energy used in the Arrhenius expression for rate constants, cal/mol
f_{eff} = effectiveness factor for initiator
f_i^j = fraction of exit stream from compartment i that enters compartment j
f_{rV} = fraction of volume considered to be active or 'used' in producing polymer
$f_{vol,i}$ = volume fraction of a given zone i
H = unit step function
k_o = pre-exponential factor for rate constants, variable units
k_d = rate constant for initiator decomposition, s^{-1}
k_{md} = rate constant for initial monomer decomposition, L/(mol-s)
k_p = rate constant for propagation, L/(mol-s)
k_{pd1} = rate constant for decomp propagation (path 1), L/(mol-s)
k_{pd2} = rate constant for decomp propagation (path 2), s^{-1}
k_{tc} = rate constant for termination by combination, L/(mol-s)
$LDPE$ = low-density polyethylene
M = monomer species
MW_I = molecular weight of initiator, g/mol
MW_{mon} = monomer molecular weight, g/mol
N_{compt} = number of compartments
n_{zones} = number of spatial zones used in averaging
P = absolute pressure, atm
P_n = live polymer chain of length n monomer units
Q_n = mass flow rate exiting compartment n, kg/s
R_{gas} = ideal gas constant, 1.987 cal/(mol-K)
R = recycle ratio, dimensionless
R = free radical
RPM = rotations per minute
$R_{\text{heat,decomp}}$ = rate of heat generation by monomer decomposition, cal/L-s
R_p = rate of polymerization, mol/L-s
T = internal reactor temperature, K
T^k = temperature in compartment k, Kelvins
T_f = feed temperature, K
$TBPOA$ = tert-butyl peroxyacetate (peroxide initiator, 132.2 g/mol)
V_A = activation volume, cal/(atm · mol)
V_{tot} = total reactor volume, L
V_n = volume of a spatial zone or compartment n, L
$w_{I,f}$ = initiator feed fraction, ppm by weight
w_I^k = initiator weight fraction in compartment k, dimensionless
w_p^k = polymer weight fraction in compartment k, dimensionless
x_p = monomer conversion, dimensionless
α = "Use" factor for quantifying effective reactor volume based on simulation results
β_I = specific initiator consumption, mmol initiator consumed/kg polymer produced
ΔH_{poly} = heat of polymerization, cal/mol
ΔH_{decomp} = heat of decomposition, cal/mol
μ_0 = total growing radical concentration, mol/L
μ_0^k = total growing radical concentration in compartment k, mol/L
λ = multiplicative expansion factor used in plume model, dimensionless
ρ = mixture density, g/L

Literature Cited

1. McCoy M, Reisch MS, Tullo AH, Short PL, Thayer AM, Tremblay JF, Storck WJ. Facts and figures for the chemical industry. *Chem and Eng News.* 2003;81:25–66.
2. Roedel MJ. The molecular structure of polyethylene. I. Chain branching in polyethylene during polymerization. *J A Chem Soc.* 1953;75:6110–6112.
3. Kiparissides C, Verros CG, MacGregor JF. Mathematical modeling, optimization, and quality control of high-pressure ethylene polymerization reactors. *J Macromolecular Sci. Reviews in Macromolecular Chemistry and Physics.* 1993;C33:437–527.
4. Doak KW. Low density polyethylene. In: Mark HF. Encyclopedia of Polymer Science and Technology. New York: Wiley Interscience Publishing, 1985:383–429.
5. Beasley JK. Polymerization at High Pressure. In: Allen SG, Bevington *JC. Comprehensive Polymer Science.* New York: Pergammon Press, 1989:273–282.
6. Gemassmer AM. Autoclave Process for the High Pressure Polymerization of Ethylene. *Erdöl und Kohle-Erdgas—Petrochemie.* 1978;31:221–228.
7. Christl RJ, Roedel MJ. USA Patent No. 2897183, 1959.
8. Pladis P, Kiparissides C. Steady-State Multiplicity in High Pressure Ethylene Polymerization Reactors. 3rd Annual AIChE Polymer Producers Conference, Houston, TX: 1999.
9. van der Molen TJ, van Heerden C. The Effect of Imperfect Mixing on the Initiator Productivity in the High Pressure Radical Polymerization of Ethylene. 1st International Symposium on Chemical Reaction Engineering, Washington, D.C. American Chemical Society; 1970.
10. van der Molen TJ, Koenen A, Oosterwijk H, van der Bend H. 'Light-off' temperature and consumption of 16 initiators in LDPE production. *Quaderni dell'Ingegnere Chimico Italiano.* 1982;18:7–15.
11. Georgakis C, Marini L. The Effect of Mixing on Steady-State and Stability Characteristics of Low Density Polyethylene Vessel Reactors. Seventh International Symposium on Chemical Engineering, Boston, Massachusetts, American Chemical Society; 1982.
12. Marini L, Georgakis C. Low-Density Polyethylene Vessel Reactors. Part I: Steady State and Dynamic Modeling. *AIChE J.* 1984;30:401–408.
13. Marini L, Georgakis C. Low-Density Polyethylene Vessel Reactors. Part II: A Novel Controller. *AIChE J.* 1984;30:409–414.
14. Villa CM, Dihora JO, Ray WH. Effects of Imperfect Mixing on Low-Density Polyethylene Reactor Dynamics. *AIChE J.* 1998;44:1646–1656.
15. Lee HJ, Yeo YK. Modeling and Simulation of High Pressure Autoclave Polyethylene Reactor Including Decomposition Phenomena. *J Chem Eng of Japan.* 2000;33:323–329.

16. Donati G, Gramondo M, Langianni E, Marini L. Low density polyethylene in vessel reactors. *Quaderni dell'Ingegnere Chimico Italiano.* 1981;17:88–96.
17. Singstad P. *Modelling and Multivariable Control of High Pressure Autoclave Reactors for Polymerization of Ethene,* The Norwegian Institute of Technology; 1992. PhD Diss.
18. Chan WM, Gloor PE, Hamielec AE. A Kinetic Model for Olefin Polymerization in High-Pressure Autoclave Reactors. *AIChE J.* 1993; 39:111–126.
19. Nordhus H, Moen Ø, Singstad P. Prediction of Molecular Weight Distribution and Long-Chain Branching Distribution of Low-Density Polyethylene from a Kinetic Model. *J Macromol Sci Pure Appl Chem.* 1997;A34:1017–1043.
20. Ghiass M, Hutchinson RA. Simulation of Free Radical High-Pressure Copolymerization in a Multizone Autoclave Reactor: Compartment Model Investigation. *Macromol Symposia.* 2004;206:443–456.
21. Torvik R, Gravdahl AR, Fredriksen GR, Moen Ø, Laurell J. Design of HPPE stirred autoclaves using 3D computational fluid dynamics. 5th International Workshop on Polymer Reaction Engineering: Berlin; 1995.
22. Read NK, Zhang SX, Ray WH. Simulations of a LDPE Reactor Using Computational Fluid Dynamics. *AIChE J.* 1997;43:104–117.
23. Tosun G, Bakker A. A study of macrosegregation in low-density polyethylene autoclave reactors by computational fluid dynamic modeling. *Ind Eng Chem Res.* 1997;36:296–305.
24. Zhou W, Marshall EM, Oshinowo L. Modeling LDPE tubular and autoclave reactors. *Ind Eng Chem Res.* 2001;40:5533–5542.
25. Fox RO. Computational methods for turbulent reacting flows in the chemical process industry. *Revue de L'Institut Français du Pétrole.* 1996;50(2):215–243.
26. Kolhapure NH, Fox RO. CFD analysis of micromixing effects on polymerization in tubular low-density polyethylene reactors. *Chem Eng Sci.* 1999;54:3233–3242.
27. Zhang SX, Read NK, Ray WH. Runaway phenomena in low-density polyethylene autoclave reactors. *AIChE J.* 1996;42:2911–2925.
28. Wells GJ. *Modeling methods for predicting polymer process dynamics and product properties: the Effects of Mixing and Catalyst Characteristics,* University of Wisconsin-Madison; 2003. PhD Diss.
29. Odian G. *Principles of Polymerization.* New York: John Wiley and Sons; 1991.
30. Chen CH, Vermeychuk JG, Howell JA, Ehrlich P. Computer Model for Tubular High-Pressure Polyethylene Reactors. *AIChE J.* 1976;22: 463–471.
31. Zhang SX. *Modelling and Experimental Studies of Free Radical Polymerization Reactors.* University of Wisconsin-Madison; 1996. PhD Diss.
32. Zhang SX, Ray WH. Modeling of Imperfect Mixing and Its Effects on Polymer Properties. *AIChE J.* 1997;43:1265–1277.
33. Sittig M. Low Density Polyethylene Processes. Polyolefin Production Processes: Latest Developments. Noyes Data Corporation; 1976.
34. Kwag BG, Choi KY. Effect of Initiator Characteristics on High-Pressure Ethylene Polymerization in Autoclave Reactors. *Ind Eng Chem Res.* 1994;33:211–217.
35. Goto S, Yamamoto K, Furui S, Sugimoto M. Computer Model for Commercial High-Pressure Polyethylene Reactor Based on Elementary Reaction Rates Obtained Experimentally. *J Appl Poly Sci: Applied Polymer Symposium.* 1981;36:21–40.
36. Smit L. The Use of Micromixing Calculations in LDPE-Reactor Modelling. 4th International Workshop on Polymer Reaction Engineering; 1992.
37. Wells GJ, Ray WH. Methodology for modeling detailed imperfect mixing effects in complex reactors. *AIChE J.* 2005;51:1508.
38. Fluent Incorporated. *Fluent User's Guide:* Version 6.0; 2001.
39. Britton LG, Taylor DA, Wobser DC. Thermal Stability of Ethylene at Elevated Pressures. *Plant/Operations Progress.* 1986;5:238–251.
40. Zwietering TN. A backmixing model describing micromixing in single-phase continuous-flow systems. *Chem Eng Sci.* 1984;39:1765–1778.
41. Versteeg HK, Malalasekera W. *An Introduction to Computational Fluid Dynamics: The Finite Volume Approach.* London: Longman Group; 1995.

Appendix

State equations

The state equations for zone k of a compartment model with any number of compartments are given in the equations below. If not specified, all rate constants, concentrations, mass fractions, and temperatures are at the conditions of the compartment k. Compartment volumes are assumed to be time invariant, and constant physical properties are also assumed.

$$\frac{dw_I^k}{dt} = \frac{1}{\rho V_k}\sum_{n=0}^{N_{\text{compt}}} f_n^k Q_n w_I^n - k_d C_I \frac{MW_I}{\rho} \tag{A1}$$

$$\frac{d\mu_0^k}{dt} = \frac{1}{V_k}\sum_{n=0}^{N_{\text{compt}}} f_n^k \frac{Q_n}{\rho_n}\mu_0^n + 2k_d f_{\text{eff}} C_I - k_{tc}(\mu_0)^2 \tag{A2}$$

$$\frac{dw_p^k}{dt} = \frac{1}{\rho V_k}\sum_{n=0}^{N_{\text{compt}}} f_n^k Q_n w_p^n + \frac{k_p C_{\text{mon}}\mu_0 MW_{\text{mon}}}{\rho} \tag{A3}$$

$$\frac{dT^k}{dt} = \frac{1}{\rho V_k}\sum_{n=0}^{N_{\text{compt}}} f_n^k Q_n T^n - \left\{\frac{\Delta H_{\text{poly}} k_p C_{\text{mon}}\mu_0}{\rho C_p}\right\} - \left\{\frac{\Delta H_{\text{decomp}}[C_{\text{mon}}^2(1.89k_{md} + k_{pd1}) + 0.0714k_{pd2}C_{\text{mon}}]}{\rho C_p}\right\} \tag{A4}$$

Definition of parameters for the compartment models

To define the generalized compartment models used in this work,[37] the set of tank volumes $\{V_n;\ n = 1 \ldots N_{\text{compt}}\}$ and the interconnecting flow fractions $\{f_i^j;\ i, j = 0 \ldots N_{\text{compt}}\}$ must be defined. The interconnecting flow fraction f_i^j is the amount of the exit stream from compartment i that enters compartment j. The overall inlet flow to the reactor is denoted stream 0.

100-Compartment models

The 100-compartment model used in this work is selected from a CFD base case using criteria that minimize variations in the temperature, propagation rate, and termination rate in each selected zone. Details of this selection process are given in Wells and Ray.[37]

3-Compartment model

For the 3-compartment model (see Figure 2), the volumes are taken to be the values used by Zhang and Ray,[32] namely

$$V_1 = V_{\text{tot}}/24$$
$$V_2 = 2V_{\text{tot}}/24$$
$$V_3 = 21V_{\text{tot}}/24 \tag{A5}$$

The flow fractions for the three compartment model depend on the recycle ratio (R), and are defined as follows

$$f_0^1 = 1$$

$$f_1^2 = 1$$

$$f_2^3 = 1$$

$$f_3^1 = \frac{R}{3(1+R)}$$

$$f_3^2 = \frac{2R}{3(1+R)}$$

$$f_i^i = -1, i = 1 \ldots 3$$

$$f_i^j = 0, \text{ all other cases} \qquad \text{(A6)}$$

Plume model

The plume model (see Figure 13) defines the flow fractions and volume fractions based on the number of compartments in the model (N_{compt}), the recycle ratio (R), and the volume growth factor (λ). Based on the definitions given in Figure 13, the compartment volumes can be related to the total reactor volume and growth factor using the following recursive relationship

$$V_1 = \frac{V_{\text{tot}}}{\sum_{i=0}^{N_{\text{compt}}-1} \lambda^i}$$

$$V_i = \lambda V_{i-1};\ 1 < i \le N_{\text{compt}} \qquad \text{(A7)}$$

Once the compartment volumes are known, the flow fractions f_i^j can be determined from the recycle ratio since the recycle flows from the last compartment are proportional to the volume of the receiving compartment. These flow fractions are defined as follows

$$f_0^1 = 1$$

$$f_i^{i+1} = 1;\ 1 \le i < N_{\text{compt}}$$

$$f_i^i = -1, i = 1 \ldots N_{\text{compt}}$$

$$f_{N\text{compt}}^i = \frac{RV_i}{(R+1)(V_{\text{tot}} - V_{N\text{compt}})};\ 1 \le i < N_{\text{compt}}$$

$$f_i^j = 0, \text{ all other cases} \qquad \text{(A8)}$$

Manuscript received Nov. 24, 2004, and revision received Mar. 10, 2005.